

Parvalbumin and Calbindin Expression in Parallel Thalamocortical Pathways in a Gleaning Bat, *Antrozous pallidus*

Heather Martin del Campo, Kevin Measor, and Khaleel A. Razak*

Department of Psychology and Graduate Neuroscience Program, University of California, Riverside, California 92521

ABSTRACT

The pallid bat (*Antrozous pallidus*) listens to prey-generated noise to localize and hunt terrestrial prey while reserving echolocation to avoid obstacles. The thalamocortical connections in the pallid bat are organized as parallel pathways that may serve echolocation and prey localization behaviors. Thalamic inputs to the cortical echolocation call- and noise-selective regions originate primarily in the suprageniculate nucleus (SG) and ventral division of medial geniculate body (MGBv), respectively. Here we examined the distribution of parvalbumin (PV) and calbindin (CB) expression in cortical regions and thalamic nuclei of these pathways. Electrophysiology was used to identify cortical regions selective for echolocation calls and noise. Immunohistochemistry was used to stain for PV and CB in the auditory cortex and MGB. A higher percentage (relative

to Nissl-stained cells) of PV⁺ cells compared with CB⁺ cells was found in both echolocation call- and noise-selective regions. This was due to differences in cortical layers V–VI, but not layers I–IV. In the MGB, CB⁺ cells were present across all divisions of the MGB, with a higher percentage in the MGBv than the SG. Perhaps the most surprising result was the virtual absence of PV staining in the MGBv. PV staining was present only in the SG. Even in the SG, the staining was mostly diffuse in the neuropil. These data support the notion that calcium binding proteins are differentially distributed in different processing streams. Our comparative data, however, do not support a general mammalian pattern of PV/CB staining that distinguishes lemniscal and nonlemniscal pathways. *J. Comp. Neurol.* 522:2431–2445, 2014.

© 2014 Wiley Periodicals, Inc.

INDEXING TERMS: echolocation; sound localization; calcium binding proteins; auditory cortex; medial geniculate body; parallel pathways

Parvalbumin (PV) and calbindin (CB) are fast cytosolic calcium buffers that have differential distributions in different regions/nuclei of sensory pathways (Baimbridge et al., 1992; Bennett-Clarke et al., 1992; Hof et al., 1999; Rausell and Jones, 1991; Rogers et al., 1990). The functional roles of neurons containing these proteins are only beginning to be identified (Sohal et al., 2009; Wu et al., 2008). These proteins have served as useful markers in neuroanatomical studies because of the differential expression patterns. For example, there is a complementary expression pattern of PV and CB in the auditory thalamocortical system of some mammalian species. In the rabbit and in rodents, the ventral medial geniculate body (MGBv) and dorsal MGB (MGBd) divisions of the auditory thalamus express primarily PV and CB, respectively (Cruikshank et al., 2001; de Venecia et al., 1995, 1998). In the macaque monkey as well, MGBv is distinguished by more PV⁺ cells than

CB⁺ cells (Jones et al., 1995; Molinari et al., 1995). In the mouse and macaque auditory cortex, PV and CB expression can distinguish primary from secondary auditory fields (Cruikshank et al., 2001; Kosaki et al., 1997; Molinari et al., 1995). These data suggest a mammalian plan of complementary PV/CB expression in the lemniscal/nonlemniscal auditory pathways. However, in the macaque MGBd, both PV and CB are

H. Martin Del Campo and K. Measor contributed equally to this work.

Grant sponsor: National Institute of Deafness and Other Communication Disorders; Grant number: R03 DC009882; Grant sponsor: National Science Foundation; Grant number: IOS-1252769.

*CORRESPONDENCE TO: Khaleel A. Razak, Department of Psychology, University of California, 900 University Avenue, Riverside, CA 92521. E-mail: khaleel@ucr.edu

Received May 31, 2013; Revised January 10, 2014; Accepted January 13, 2014.

DOI 10.1002/cne.23541

Published online January 17, 2014 in Wiley Online Library (wileyonlinelibrary.com)

© 2014 Wiley Periodicals, Inc.

strongly expressed in cells. Studies of bats also show divergence from a general plan. In the mustached bat, PV and CB are strongly expressed in both MGBd and MGBv (Zettel et al., 1991). In the horseshoe bat, both PV and CB are expressed strongly in the MGBv (Vater and Braun, 1994). PV/CB expression patterns may therefore distinguish species-specific processing streams as opposed to being biochemical markers of lemniscal/nonlemniscal pathways.

The goal of this study was to examine expression patterns of calcium binding proteins in a bat species in which different thalamocortical pathways may serve two different behaviors. PV and CB expression pattern was investigated in the MGB and auditory cortex of the pallid bat (*Antrozous pallidus*). Unlike the mustached and horseshoe bats, which use echolocation primarily to hunt aerial prey, the pallid bat belongs to a small group of bats called *gleaners*, which hunt terrestrial prey (Barber et al., 2003; Bell, 1982; Fuzessery et al., 1993). Gleaners depend, at least partially, on listening to prey-generated sounds to hunt and are found across families, suggesting convergent evolution of this behavior. Pallid bats listen to prey-generated noise to localize and hunt prey such as crickets and scorpions while reserving echolocation for obstacle avoidance.

The auditory cortex of the pallid bat is dominated by two adjacent, and mostly segregated, regions with response selectivity for the sounds used in echolocation (60→30 kHz downward frequency modulated sweeps, 2–6 msec) and prey localization (5–35 kHz noise transients; Razak, 2011; Razak and Fuzessery, 2002, 2006). Both cortical regions are overlain on a tonotopic map representing the species-specific audible range (~5–70 kHz). In addition, neurons in both regions have short latency responses and narrow tuning, suggesting that they are both part of the primary auditory cortex (A1). However, only one half of this tonotopic map receives input from the MGBv (Razak and Fuzessery, 2010; Razak et al., 2007, 2009). The noise-selective region (tuning between 5 and 35 kHz) receives input from the MGBv. The echolocation call-selective region (tuning between 30 and 70 kHz) receives most input from the supragenulate nucleus (SG) of the MGBd. These data suggest that the thalamocortical connections emphasize segregation of the two pathways in the pallid bat, perhaps to enhance segregated processing of two sound streams (FM and noise) that likely co-occur in natural hunting situations (Barber et al., 2003). This study tested the hypothesis that these two parallel processing streams show different patterns of PV/CB expression.

Data show that the expression of PV/CB in the pallid bat MGB is different from that in any other species examined, including other bats. PV is expressed only in

the SG of the pallid bat MGB. CB is expressed across the MGB, but in a larger percentage of cells in the MGBv compared with the SG. In A1, PV is expressed in a similar percentage of cells in the noise- and echolocation call-selective region. More PV⁺ than CB⁺ cells are present in A1.

MATERIALS AND METHODS

Adult pallid bats were netted in Arizona, California, New Mexico, or Texas and held in a 11 × 14 ft room at the University of California, Riverside. The bats were able to fly in this room and were provided crickets/mealworms and water ad libitum. The room was maintained on a reversed 12:12-hour light:dark cycle. All procedures followed the animal welfare guidelines required by the National Institutes of Health and were approved by the Institutional Animal Care and Use Committee.

General overview of procedure

Single- and multiunit electrophysiology was used to generate a coarse map of the right auditory cortex in terms of characteristic frequencies (CF). A fluorescent marker was placed in putative FM- and/or noise-selective region identified based on CF. In sections containing the cortical fluorescent marker, PV- and CB-stained cells were counted in the opposite (left) hemisphere at locations homotopic to the dye location. In the MGB, PV and CB staining was compared between different divisions identified based on Nissl staining.

Surgical procedures for cortical electrophysiology

Isoflurane was used to anesthetize the bats briefly for injections of sodium pentobarbital. Recordings were obtained from bats anesthetized with an i.p. injection of pentobarbital sodium (30 µg/g body wt) and acepromazine (2 µg/g body wt). Both male and female bats were used. Because the goal of electrophysiology was to simply identify tonotopy to target dye marking, it is unlikely that the pentobarbital anesthesia had a significant impact on the observed results. To expose the auditory cortex, the head was held in a bite bar, a midline incision was made in the scalp, and the muscles over the dorsal surface of the skull were reflected to the sides. The front of the skull was scraped clean and a layer of glass microbeads applied, followed by a layer of dental cement. The bat was then placed in a Plexiglas holder. A cylindrical aluminum head pin was inserted through a cross bar over the bat's head and cemented to the previously prepared region of the skull. This pin served to hold the bat's head secure during the recording

session. The location of A1 was determined relative to the rostrocaudal extent of the midsagittal sinus, the distance laterally from the midsagittal sinus, and the location of a prominent lateral blood vessel that travels parallel to the midsagittal sinus (Razak and Fuzessery, 2002). The size of the exposure was usually $\sim 2 \text{ mm}^2$. Exposed muscle was covered with petroleum jelly, and exposed brain surface was covered with silicone oil to prevent desiccation.

Recording procedures

Electrophysiological recordings were used to identify and mark putative noise- and/or FM sweep-selective regions of the pallid bat auditory cortex. Several previous studies have shown that the noise-selective region is tonotopically organized with CF between ~ 5 and 30 kHz and robust responses to broadband noise (Razak, 2011, 2012a; Razak and Fuzessery, 2002, 2007). The FM sweep-selective region is also tonotopically organized with CF between ~ 30 and 60 kHz and direction- and rate-selective responses to the 60 \rightarrow 30 kHz FM sweeps used by the pallid bat to echolocate (Razak, 2012b; Razak and Fuzessery, 2002, 2006, 2009). Therefore, the focus was to obtain a map of CFs and to place dye to mark the high and/or low CF cortex that corresponds to FM- and/or noise-selective region. In a number of sites, the intuition based on CF regarding noise vs. FM sweep selectivity was verified by recording responses to these sounds as well.

Experiments were conducted in a warm (80°F), sound-proofed chamber lined with anechoic foam (Gretch-Ken Industries). All recordings were obtained from the right hemisphere. Bats were kept anesthetized throughout the course of the experiments with additional pentobarbital sodium (one-third of the presurgical dose) injections. Acoustic stimulation and data acquisition were driven by custom-written software (Batlab; written by Dr. Don Gans, Kent State University) and a Microstar digital signal-processing board. Programmable attenuators (PA5; Tucker-Davis Technologies) allowed control of sound intensities before amplification by an integrated amplifier (Yamaha AX430) or a power amplifier (Parasound HCA1100).

Extracellular single- or multiunit recordings were obtained using glass electrodes (1 M NaCl, 2–10 M Ω impedance) at depths between 200 and 600 μm . Penetrations were made orthogonal to the surface of the cortex. Action potentials were amplified by a Dagan extracellular preamplifier (2400A) and a spike signal enhancer (FHC) and bandpass filtered (0.3–3 kHz; Krohn-Hite). Waveforms and peristimulus time histograms were stored by using the Microstar DSP board and Batlab software. Single-unit recordings were

identified based on window discrimination and the consistency of action potential amplitude and waveform displayed on an oscilloscope.

Stimuli were presented with an LCY-K100 ribbon tweeter (Madisound, Madison, WI) fitted with a funnel that was inserted into the left pinna (contralateral to recorded cortex). The amplifier-speaker-funnel frequency-response curve measured with a 1/4-in microphone (Briel and Kjaer) was flat within $\pm 3 \text{ dB}$ for frequencies from 8 to 35 kHz. The decline in response at higher frequencies was smooth up to 70 kHz at a fall-off rate of $\sim 20 \text{ dB/octave}$. In two experiments, the FM sweep-selective region was identified by using a free-field speaker (LCY-K100 ribbon tweeter) placed at 0° azimuth and elevation with respect to the bat's snout at a distance of 40 cm.

Upon penetration of the cortical surface with the electrode, pure tones (5–60 kHz, 1 msec rise/fall time, 5–10 msec duration), downward and upward FM sweeps (30–70 kHz, 20–40 kHz bandwidth, 2 msec/rise/fall time, 2–30 msec duration), and noise (5–40 kHz broadband, 1 msec rise/fall time, 5–10 msec) were played at a repetition rate of 1 Hz and at different intensities (10–70 dB) to search for sound-driven responses. When robust multiunit responses or isolated single-unit responses to one or more of these stimuli were obtained, the CF was determined. CF was defined as the tone frequency that elicited action potentials to at least five successive stimulus repetitions at the lowest intensity. This intensity was noted as the minimum threshold (MT) of the neuron. A similar procedure was used to map the CFs across the cortex.

Dye injection

A fluorescent dye was injected to mark the low-CF (5–30 kHz) and/or high-CF (30–60 kHz) cortical regions. Tips of glass electrodes ($\sim 10 \mu\text{m}$ diameter) were capillary-filled with 20 mg/ml dextran tetramethyl rhodamine (Invitrogen, Carlsbad, CA; diluted with 0.9% normal saline) and back-filled with 1 M NaCl. The dye was injected using a Midgard precision current source (Stoelting, Wood Dale, IL) with 7 seconds on–7 seconds off current stimulus of $+4 \mu\text{A}$. The duration of injection was 5 minutes at a depth of ~ 300 –600 μm . After histological processing (details below), dye injection sites were viewed with a Nikon Eclipse 80i microscope with epifluorescent light filters. Images were taken with a Nikon Digital Sight camera.

Immunohistochemistry

After a lethal injection of sodium pentobarbital (125 mg/kg), bats were transcardially perfused with a peristaltic pump (Fisher Scientific, Fair Lawn, NJ) with

0.1 M PBS, followed by 4% paraformaldehyde (0.1 M PB, pH 7.4). The brains were immediately removed, postfixed overnight (~15–20 hours) in 4% paraformaldehyde, and cryoprotected in 30% sucrose until sinking. Brains were coronally sectioned at 40 μ m on a cryostat. Immunohistochemistry was carried out with free-floating sections at room temperature with agitation unless otherwise indicated. Sections were pretreated in 0.5% H₂O₂ (in 0.1 M PBS, pH 7.4, 30 minutes) to reduce endogenous peroxidase activity, then rinsed with 0.3% Tween-20 detergent (in 0.1 M PBS, 3 \times 10 minutes) and blocked with 6.7% goat normal serum (s-1000, Vector, Burlingame, CA; in 0.1 M PBS, 2–3 hours). Sections were incubated at 4°C in a solution containing either rabbit anti-PV (1:5,000, PV-25; Swant, Bellinzona, Switzerland) or mouse anti-CB (1:5,000, D-28k; Swant), 2% goat normal serum, and 0.3% Triton X-100 (in 0.1 M PBS, 2–4 nights).

Sections were rinsed in 0.3% Tween-20 (in 0.1 M PBS, 3 \times 10 minutes), followed by an incubation in a solution containing peroxidase-conjugated AffiniPure goat anti-rabbit IgG (H+L; 1:500; Jackson ImmunoResearch, West Grove, PA), 2% goat normal serum, and 0.3% Triton X-100 (in 0.1 M PBS, 2–3 hours). Sections

were then rinsed (in 0.1 M PBS, 3 \times 10 minutes). Staining was visualized without agitation by first preincubating the sections in 3,3'-diaminobenzidine (DAB; sk-4100; Vector) solution, followed by incubation with H₂O₂ and DAB. Sections were rinsed in dH₂O (2 \times 10 minutes), transferred to 0.1 M PBS, mounted on gelatin-coated slides, air dried, and coverslipped with DPX mounting medium (Electron Microscopy Sciences, Fort Washington, PA).

Antibody characterization

An antibody against calbindin D-28k (300; Swant) was examined for antigen specificity by using Western blot analysis (Fig. 1). Brain extracts from the pallid bats were separated by SDS-PAGE protein separation, transferred to a nitrocellulose membrane, and then probed with the antibody. A single band at 28 kDa was observed, confirming a high level of specificity in the pallid bat. An antibody against parvalbumin (PV25; Swant) could not be validated in the pallid bat because, according to the manufacturer, the PV25 antibody does not recognize the antigen after SDS-gel electrophoretic separation of brain extracts (Swant product specification sheet). We have used this antibody in a previous study (Martin del Campo et al., 2012) in the mouse auditory cortex and reported similar cortical staining patterns. The manufacturers report that staining is absent in PV KO mouse brain tissue. As far as the authors are aware, there have been no examples of cross-reaction with other antigens on record. Additional information on the antibodies used is provided in Table 1.

Image analysis, counting, and data representation

Nissl⁺, CB⁺, and PV⁺ cells were counted in the left hemisphere of each cortex. The general location of the auditory cortex was identified based on hippocampal landmarks. More accurate location of the FM sweep-and/or noise-selective regions in the right hemisphere was accomplished based on the dye injection (Fig. 2A,B). Homotypic regions in the left hemisphere were chosen for counting (Fig. 2C,D). Adjacent sections were counted for CB⁺, PV⁺, and Nissl⁺ cells.

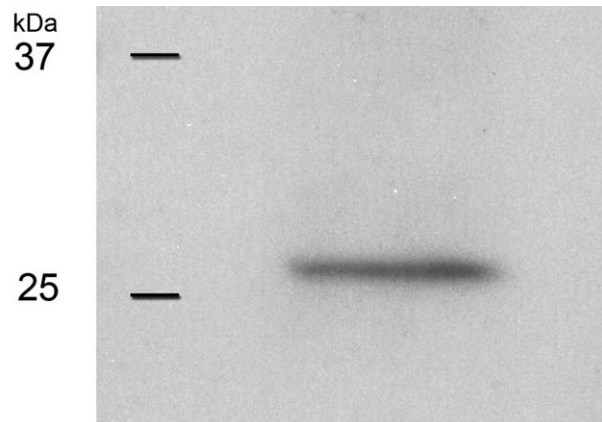


Figure 1. Specificity of calbindin D28K antibody shown by Western blotting of pallid bat brain tissue after electrophoretic SDS-PAGE protein separation. Position of molecular mass markers in kilodaltons reported is at left.

TABLE 1.
Antibodies Used in This Study

Antibody	Supplier	Type	Host	Dilution	Immunogen
Anticalbindin D-28K ¹	Swant, 300, lot 07(F)	Monoclonal IgG1	Mouse	1:5,000	Calbindin D28K purified from chicken gut
Antiparvalbumin ²	Swant, PV25, lot 5.10	Polyclonal	Rabbit	1:5,000	Parvalbumin purified from rat muscle

¹Antibody was validated by Western blot assay with purified pallid bat cortex (Fig. 1).

²Validation was not possible by Western blot assay (manufacturer's information). The authors previously used PV25 antibody in mouse cortex and had staining patterns that were similar to those in the present study in the pallid bat (Martin del Campo et al, 2012).

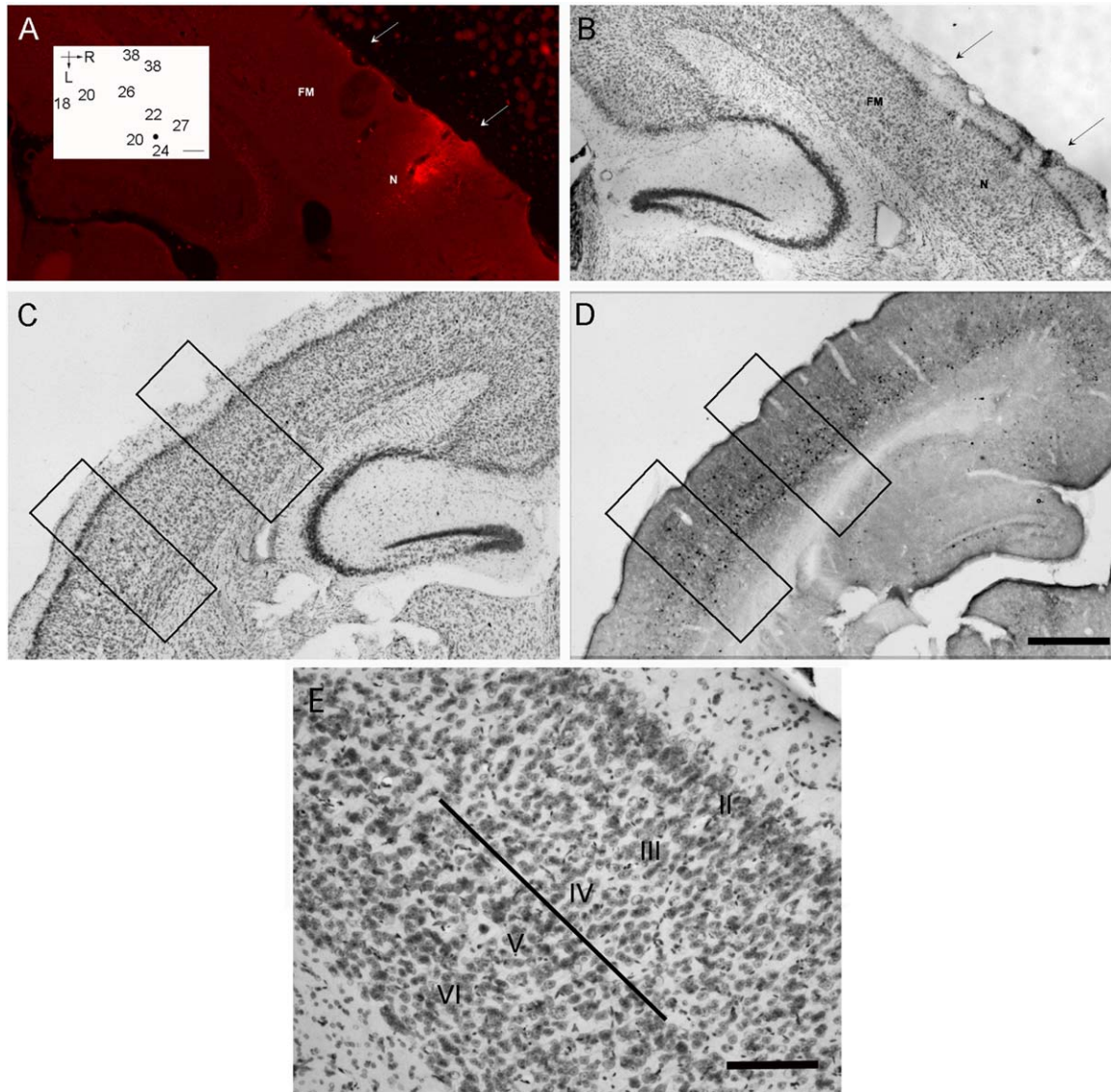


Figure 2. Illustration of the main methods used in this study. **A:** Photomicrograph of a coronal section through the frequency-modulated (FM) sweep- and noise (N)-selective regions of the pallid bat auditory cortex. Fluroruby was used to mark the N region. These regions were identified by using electrophysiology. The **inset** shows the map of characteristic frequencies (CF) identified using electrophysiology from the right auditory cortex (pallid bat PAL024). The black circle shows the site of fluroruby injection to mark the noise-selective neurons (CFs ~20–27 kHz). The neurons located more medially with CF ~38 kHz are in the FM sweep selective region. R, rostral; L, lateral. **B:** Photomicrograph of the section located adjacent to the section shown in A. This section was Nissl stained. **C:** The contralateral side of the same section shown in B was used to identify layers and count Nissl-stained cells in the putative FM and N region. The assumption that the locations of FM- and N-selective regions were symmetrical across the midline was made. Nissl-stained cell counts were determined in 400- μ m-wide rectangles spanning the layers of the cortex. **D:** Photomicrograph of a PV-stained section located adjacent (40 or 80 μ m) to the Nissl-stained section. The number of PV-positive cells was counted within the 400- μ m-wide rectangles placed over the putative FM and N regions. **E:** Nissl-stained section through the FM sweep-selective region of the auditory cortex. The solid line demarcates layers IV and V to facilitate a comparison of cell counts between layers I–IV and layers V–VI. Scale bars = 500 μ m in D (applies to A–D); 200 μ m in E; ~200 μ m in inset in A. [Color figure can be viewed in the online issue, which is available at wileyonlinelibrary.com.]

NIS Elements advanced research software was used to capture 400- μ m-wide images of the auditory cortex in CB⁺, PV⁺, and Nissl⁺ sections (height from white matter to pia). The auditory cortex was divided into layers I–IV and layers V–VI based on the laminar

distribution of cells (solid line, Fig. 2E). Layer IV contains small, densely concentrated cells, and layer V contains larger, more darkly stained and sparsely spaced pyramidal cells. Based on this difference, the boundary between layers IV and V was placed between

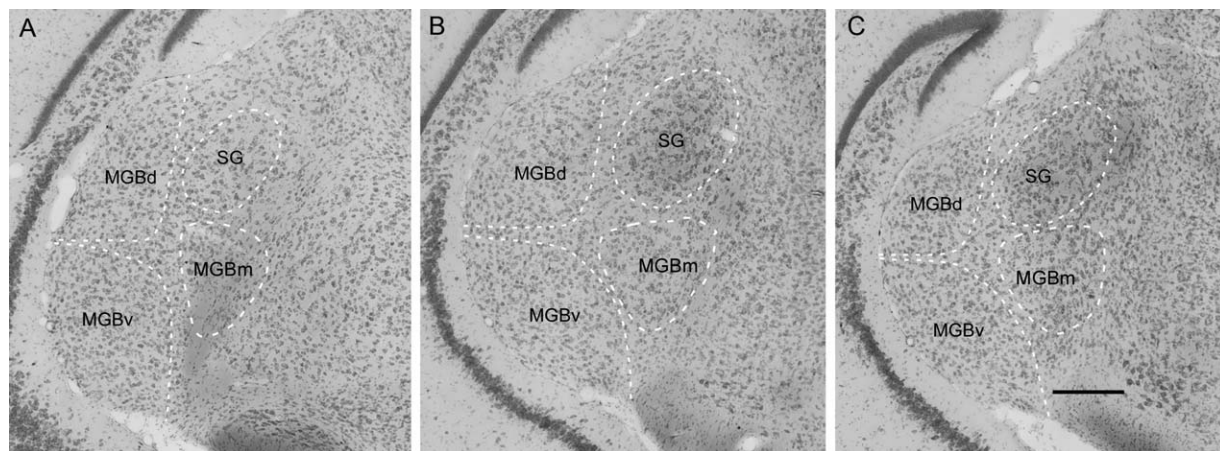


Figure 3. A–C show a rostral-to-caudal sequence of sections through the MGB of a pallid bat. The sections were at 70% (A), 40% (B), and 20% (C) rostrocaudal MGB positions (100% being most rostral). The dashed white lines demarcate the approximate boundaries of the various regions of interest in this study. Although the SG is considered a part of the MGBd, they were analyzed separately. The SG is most distinct based on large cell bodies and darker Nissl staining. Scale bar: 200 μm .

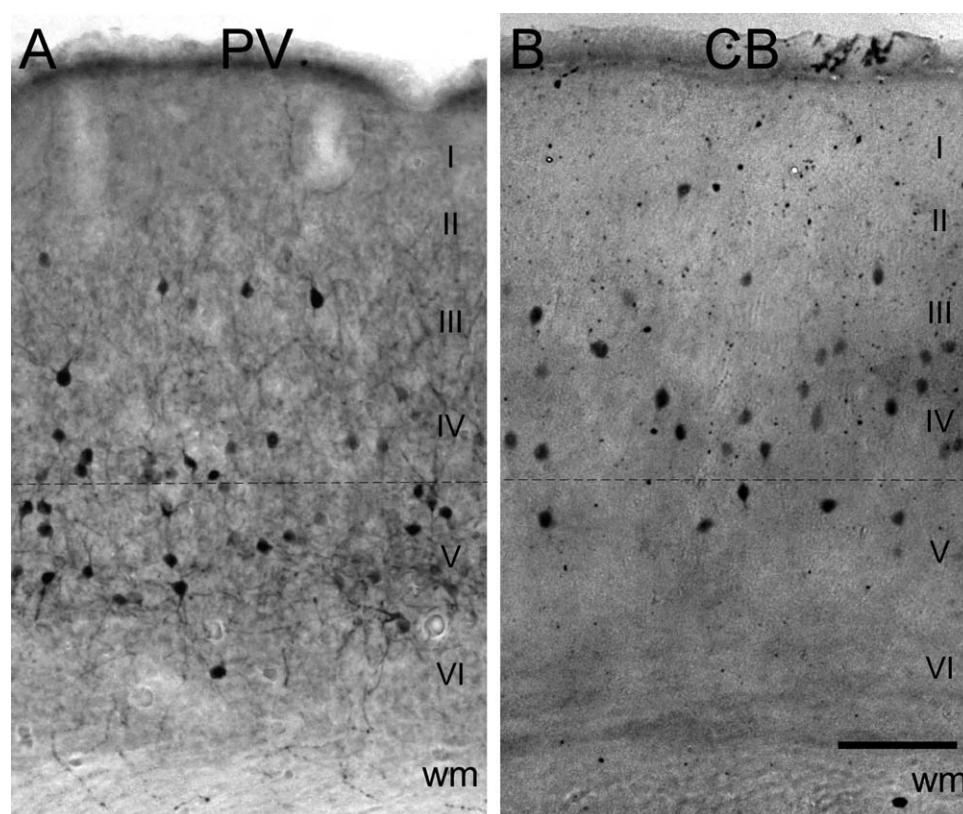


Figure 4. Example photomicrographs of PV (A) and CB (B) immunostaining in the FM sweep-selective region of the auditory cortex of the pallid bat. Dashed line is at the boundary between layers IV and V identified in a Nissl-stained adjacent section. Wm, white matter. Scale bar = 150 μm .

54% and 61% of total section height (pia to white matter) for all bats in this study. This is consistent with a previous study on the pallid bat cortex (Marsh et al., 2002), which placed the boundary at $\sim 60\%$ from the pia. The

boundary between the layers IV and V was then marked on adjacent sections stained for PV or CB to count cells positive for these calcium binding proteins in layers I–IV and layers V–VI. A finer-grained layer analysis was not possible because the boundaries between layers III–IV and layers V–VI were not consistently distinguishable with Nissl staining.

Prior to counting, images were adjusted for brightness and contrast in NIS Elements. Nissl-stained cells were counted in one of the eight randomly selected 50- μm -wide rectangles within the 400- μm image of Nissl-stained section. This count was multiplied by a factor of 8. CB^+ and PV^+ cells were counted across the entire 400- μm -wide image of CB and PV stained sections. Only those CB^+ and PV^+ cells that had intensely stained soma were included in the counts. Counting bias was avoided by counting only cells

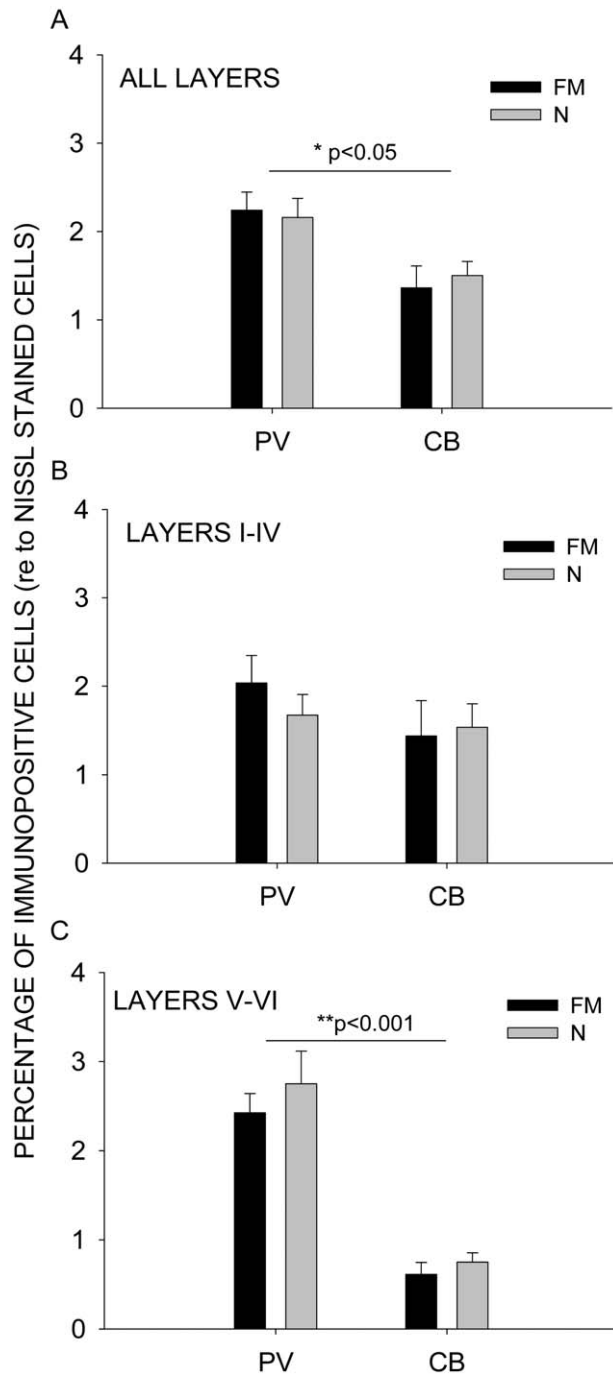


Figure 5. Distribution of parvalbumin (PV)- and calbindin (CB)-immunoreactive (IR) cells in the FM and noise regions of pallid bat auditory cortex. The data for this figure are shown in Table 2. **A:** Percentage of PV⁺ or CB⁺ cells expressed as a percentage of Nissl-stained cells across all layers of the cortex. Both FM and noise regions contain a significantly greater percentage of PV⁺ than CB⁺ cells. There was no difference in expression of either calcium binding protein across the two cortical regions. **B:** Comparison only within layers I–IV shows no difference in the percentage of PV⁺ and CB⁺ cells in either FM or noise regions. However, in layers V–VI, there was significant difference in the percentage of PV⁺ and CB⁺ neurons (**C**).

that either had their soma contained completely within the image or that fell on the left border of the image. Those cells that fell on the right border of the image were excluded from counting (Gundersen et al., 1988). Data are represented in terms of percentage of CB⁺ or PV⁺ cells relative to Nissl-stained cells.

The different divisions of the MGB were identified via Nissl staining (Fig. 3) based on the scheme of Morest (1964). Although the SG is considered a part of the MGBd, we analyzed it separately in this study because most of the echolocation pathway appears to be routed through the SG (Razak et al., 2007). In the text, *MGBd* refers to parts of this division excluding the SG. Figure 3 shows three Nissl-stained sections through the MGB arranged in a rostral-to-caudal fashion. The SG can be distinguished from the MGBv and MGBd based on darkly stained cells with larger soma. The MGBm has a broader range of cell sizes and reduced cell density. It is relatively more difficult to distinguish MGBd and MGBv based on Nissl staining. The approximate boundary between these two divisions was placed based on previous studies that used fiber staining procedures and showed that the MGBv is mostly devoid of fibers compared with the MGBd (Razak et al., 2007; Shen, 1996). It must be noted that the primary focus was on differentiating the SG from the MGBv, because these nuclei are the main sources of input to the FM sweep- and noise-selective regions of the cortex. Cell counts in the MGB were made in 100- μm^2 squares placed in the center of the dashed contours (Fig. 3) outlining each region.

RESULTS

PV expression was studied in seven bats in the MGB. In six of these bats, PV expression was also studied in the FM- and noise-selective regions of the auditory cortex. In a separate set of five bats, CB expression was studied in the MGB. For four of these bats, we also examined CB expression in the auditory cortex.

PV and CB staining in the auditory cortex

Figure 4 shows representative PV and CB staining in the auditory cortex. Intense staining of cell bodies was present for both PV and CB. The percentage of PV⁺ and CB⁺ cells relative to Nissl-stained cells was compared between the FM and the N areas and analyzed by using two-way ANOVA (cortical area \times calcium binding protein) with post hoc Tukey pairwise comparisons (Fig. 5). Table 2 shows the absolute cell counts in the sections used for the analysis. There was no difference between FM and N areas in terms of the percentage of calcium binding proteins ($P > 0.05$). However, within each area, there were more PV⁺ cells than CB⁺ cells

TABLE 2.
Quantification of CB⁺ and PV⁺ Cells in the Auditory Cortex

			All layers			Layers I-IV			Layers V-VI		
	Section ID	Region	Nissl cells	IR cells	% IR cells	Nissl cells	IR cells	% IR cells	Nissl cells	IR cells	% IR cells
PV	PAL23-1	FM	1,376	36	3	736	18	2	640	18	3
		N	1,440	30	2	728	12	2	712	18	3
	PAL23-2	FM	1,344 ¹	40	3	704 ¹	19	3	640 ¹	21	3.
		N	1,418 ¹	13	1	784 ¹	9	1	634 ¹	4	1
	PAL24-1	FM	1,200	38	3	592	23	4	608	15	3
		N	1,512	44	3	800	17	2	712	27	4
	PAL24-2	FM	1,232	38	3	560	15	3	672	23	3
		N	1,528	31	2	824	24	3	704	7	1
	PAL27-1	FM	1,288	30	2	680	22	3	608	8	1
		N	1,520	24	2	872	1	1	648	23	4
	PAL27-2	FM	1,336	36	3	616	18	3	720	18	3
		N	1,144	35	3	568	14	3	576	21	4
	PAL37-1	FM	1,376	16	1	728	8	1	648	8	1
		N	1,520	27	2	720	15	2	800	12	2
	PAL37-2	FM	1,288	16	1	624	3	1	664	13	2
		N	1,232	34	3	696	13	2	536	21	4
	PAL40-1	FM	1,136	24	2	552	9	2	584	15	3
		N	1,024	36	4	544	13	2	480	23	5
	PAL40-2	FM	1,136	16	1	528	6	1	608	10	2
		N	1,112	18	2	656	7	1	456	11	2
	PAL53-1	FM	1,376	29	2	744	12	2	632	17	3
		N	1,560	25	2	944	13	1	616	14	2
CB	PAL53-2	FM	1,328	27	2	704	5	1	624	20	3
		N	1,600	30	2	880	8	1	720	22	3
	PAL64-1	FM	1,376	4	1	736	3	1	640	1	1
		N	1,376	11	1	712	8	1	664	3	1
	PAL64-2	FM	1,496	6	1	904	1	1	592	5	1
		N	1,488	3	2	864	1	1	624	2	1
	PAL67-1	FM	1,544	3	2	872	2	1	672	1	1
		N	1,496	21	2	880	16	2	616	5	1
	PAL67-2	FM	1,608	24	2	920	20	2	688	4	1
		N	1,592	17	1	912	13	1	680	4	1
	PAL68-1	FM	1,344 ¹	11	1	704 ¹	8	1	640 ¹	3	1
		N	1,418 ¹	20	1	784 ¹	13	2	634 ¹	7	1
	PAL68-2	FM	1,344 ¹	25	2	704 ¹	20	3	640 ¹	5	1
		N	1,418 ¹	28	2	784 ¹	21	3	634 ¹	7	1
	PAL69-1	FM	1,408	24	2	768	16	2	640	8	1
		N	1,536	22	1	944	16	2	592	6	1
	PAL69-2	FM	1,344 ¹	22	2	704 ¹	18	3	640 ¹	4	1
		N	1,418 ¹	18	1	784 ¹	14	2	634 ¹	4	1

¹A few sections that would have been used for Nissl counting were damaged. Average Nissl counts of all sections corresponding to the same FM/N region and layers of the cortex were used in place of the missing counts. The percentage IR value in the table has been rounded to the closest integer, with values between 0.1% and 1% rounded to 1%.

($P < 0.05$) when the cells were counted across all six cortical layers (Fig. 5A). Analyzing granular/supragranular layers I–IV (Fig. 5B) and infragranular layers V–VI (Fig. 5C) separately indicates that the difference between PV and CB expression was mainly in the infragranular layers ($P < 0.001$) in both the FM and the N regions. There was no difference in the percentage of CB⁺ and PV⁺ cells in layers I–IV in both regions ($P > 0.05$). These data indicate that the two calcium binding proteins tested were expressed at different levels in the cortex, without a difference between functional cortical areas.

Differential staining patterns of PV and CB in the MGB

The MGBv, MGBd, and SG were analyzed for expression of CB and PV. Although the SG is generally considered a part of the MGBd, we analyzed the data separately for these two regions because the echolocation pathway is routed to a larger extent through the SG. In the text below, MGBd refers to the parts of the dorsal division excluding the SG.

Expression patterns of CB and PV in the MGB were region specific. Perhaps the most surprising finding was

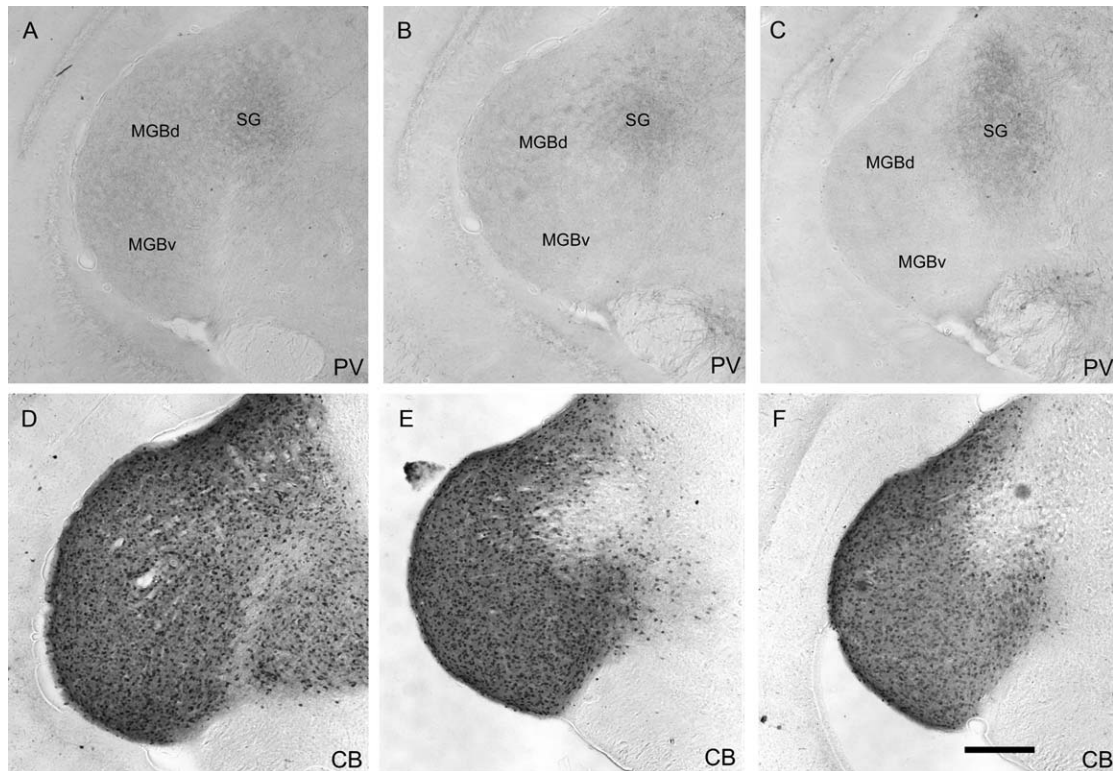


Figure 6. Parvalbumin (A–C) and calbindin (D–F) staining in the MGB suggestive of complementary expression patterns. The left to right (e.g., A–C) progression of sections for each animal is in a rostral to caudal direction. The PV- and CB-stained sections are from two different bats taken at approximately similar rostrocaudal locations of the MGB (70%, 55%, and 40% rostral to caudal). The labels indicate approximately the center of each MGB region demarcated using adjacent Nissl-stained sections. PV staining was limited to the SG, in which it was diffuse and limited mostly to the neuropil. PV staining was not discernible in the MGBd and MGBv. CB⁺ cells, in contrast, were found in all three regions analyzed. However, more caudally, there was a reduction in CB⁺ cells in the SG appearing in an essentially complementary fashion to PV staining. Scale bar = 250 μ m.

the virtual absence of PV staining in the MGBv and MGBd (Figs. 6A–C, 7A–D). Figure 6A–C shows PV staining in three sections through the MGB. Figure 7A–D shows PV expression in two other bats. Only the SG showed evidence of PV staining, and, even there, the staining was diffuse and limited to the neuropil with rare somata staining (Fig. 7B shows the section with the most number of PV⁺ SG cells in the study). MGBv and MGBd were devoid of PV-stained cells or neuropil. Figure 8 shows both MGB and cortex (note that this not auditory cortex) in the same section. Staining is visible in cortical cells and the SG but not in the MGBv or MGBd, indicating that the weak PV immunoreactivity in the MGB is not a result of potential differences in staining protocol. Given that only the rare cell body in the SG showed PV staining, percentage of PV-stained cells was not quantified.

In contrast to PV, CB immunoreactivity was present in all divisions of the MGB, albeit at different levels and in a pattern that appears complementary to PV expression. Figure 6D–F shows CB staining in the MGB.

Comparison of PV and CB staining in Figure 6 indicates the complementary patterns with more CB⁺ cells in the MGBd and MGBv than the SG and with PV staining only in the SG. Figure 7E–H shows CB staining in the MGB of two other bats. Quantification of CB⁺ cell counts relative to Nissl-stained cells supports the observation of more CB⁺ cells in the MGBd and MGBv compared with the SG (Table 3, Fig. 9). A one-way ANOVA revealed that there was no difference between the MGBv and the MGBd in the percentage of CB⁺ cells. However, the percentage of CB⁺ neurons in the SG was significantly lower ($P < 0.01$) than the other two regions. Together these data indicate differential staining patterns of PV and CB in the different regions of the MGB of the pallid bat.

DISCUSSION

The main goal of this study was to quantify PV and CB staining in parallel thalamocortical pathways: 1) the thalamic SG nucleus and its cortical projection zone,

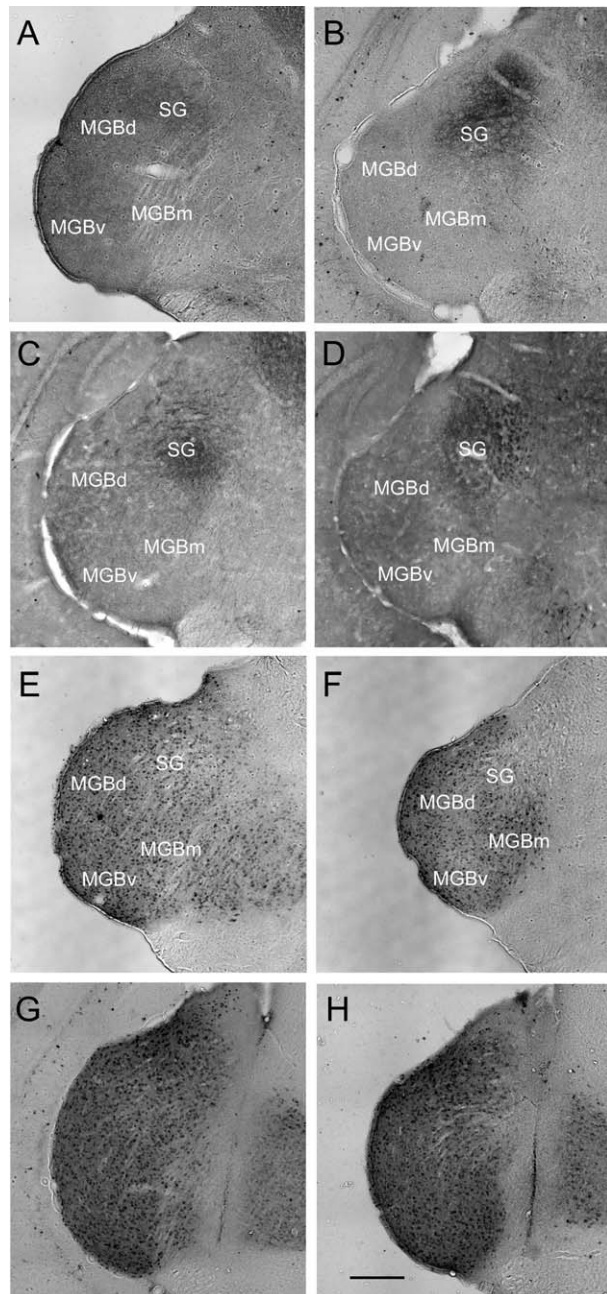


Figure 7. Additional examples of PV (A–D) and CB (E–H) staining in the MGB. Each row corresponds to two sections from the same bat, the left column being more rostral than the right. The sections are approximately at the same rostrocaudal location in the MGB. Scale bar = 250 μ m.

the FM-selective region (putative echolocation pathway), and 2) the thalamic MGBv division and its cortical projection zone, the noise-selective region (putative prey-localization pathway). There were two major findings. First, the calcium binding proteins CB and PV show differential staining patterns across the MGB (summarized in Fig. 10). CB^+ cells were present across the various divisions of the MGB but were differentially distributed.

Specifically for the functional pathways, a greater percentage of CB^+ cells was found in the MGBv compared with the SG. There was no difference between the MGBd and the MGBv. PV staining was, however, constrained to the SG and absent in the MGBv and parts of the MGBd outside the SG. Most PV expression was limited to diffuse staining of the neuropil in the SG. Second, in the auditory cortex, there was a higher percentage of PV^+ than CB^+ cells in layers V–VI but not in layers I–IV. However, this was seen in both the FM- and the noise-selective areas, with no area-specific difference. Thus, the MGB, but not cortical, expression pattern of CB/PV appears to be functional pathway specific.

The FM-selective region contains neurons tuned between 30 and 60 kHz. The majority (~70–75%) of neurons in this region are selective for the 60→30 kHz downward FM sweeps used by the pallid bat to echolocate obstacles. This form of response selectivity suggests this region's involvement in echolocation. The FM-selective region receives input mostly from the SG and none from the MGBv. The noise-selective neurons are tuned between 6 and 35 kHz. Most neurons respond robustly to 5–40 kHz noise, and this region contains a systematic map of binaural and azimuth selectivity that may be involved in localization of prey-generated noise (Razak, 2011). The noise-selective region receives most inputs from the MGBv, and none from the SG. Taken together, the pallid bat thalamocortical connections appear to emphasize functional, connectional, and molecular segregation of parallel pathways involved in two different behaviors. Such parallel processing may enhance behavioral segregation of streams of echoes and prey-generated noise that will arrive at the cochlea nearly simultaneously in typical hunting situations.

Comparison across species

MGB. Considerable species-specific differences exist in the expression patterns of PV and CB in the MGB (Fig. 11). The general trend in rodents and in the rabbit is a complementary expression pattern of PV and CB in a lemniscal/nonlemniscal or core/shell organization (Cruikshank et al., 2001; de Venecia et al., 1995; Ouda et al., 2008). PV expression is strongest in the MGBv and weak or absent in the MGBd, whereas CB expression is weak or absent in the MGBv and strong in the MGBd. The SG in the rabbit is devoid of PV expression. The SG was not explicitly identified in the rodent studies. In rodents, unlike rabbits, strong PV expression in the MGBv is limited to the neuropil, with sparse labeling of the somata. Although less specific in terms of identified MGB divisions, studies of gerbil and guinea pig MGB also support the trends observed in rabbits and

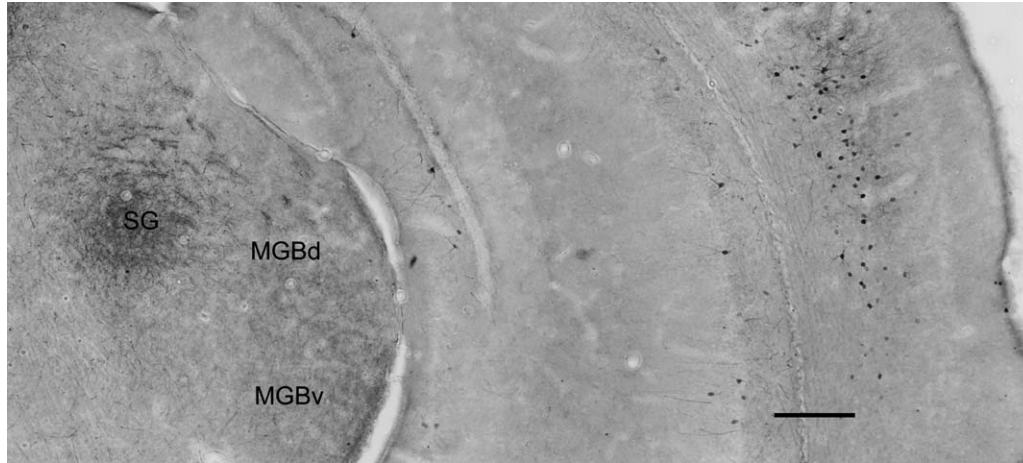


Figure 8. Photomicrograph of PV staining ($\times 10$) showing intense cell body staining in the cortex (note that this is not auditory cortex) and neuropil staining in the SG but no staining in the MGBv or the MGBd. This image illustrates the low level of PV expression in the MGB compared with the cortex in the same section. Scale bar = 250 μm .

TABLE 3.
Quantification of CB⁺ Cells in the Medial Geniculate Body

Region	Section ID	% Location ¹	Nissl cells	CB ⁺ cells	% CB ⁺ cells	CB ⁺ cells/100 μm^2
MGBv	PAL64 2-4	57	201	103	51	26
	PAL65 2-3	57	161	79	49	20
	PAL65 2-4	43	161	68	42	17
	PAL67 2-6	71	176	80	46	20
	PAL67 2-7	57	166	88	53	22
	PAL67 2-8	43	161	94	58	24
	PAL67 2-9	29	210	66	31	17
	PAL68 2-5	57	235	44	19	11
	PAL68 2-6	43	214	69	32	17
	PAL68 2-7	29	198	82	41	21
	PAL69 2-2	57	147	74	50	19
	PAL69 2-3	43	149	85	57	21
MGBd	PAL64 2-4	57	190	97	51	24
	PAL65 2-3	57	155	79	51	20
	PAL65 2-4	43	253	78	31	20
	PAL67 2-6	71	191	62	33	16
	PAL67 2-7	57	175	96	55	24
	PAL67 2-8	43	163	79	49	20
	PAL67 2-9	29	204	79	39	20
	PAL68 2-5	57	208	72	35	18
	PAL68 2-6	43	196	88	45	22
	PAL68 2-7	29	146	86	59	22
	PAL69 2-2	57	162	51	32	13
	PAL69 2-3	43	169	68	40	17
SG	PAL64 2-4	57	187	23	12	6
	PAL65 2-3	57	179	42	28	11
	PAL65 2-4	43	237	29	12	7
	PAL67 2-6	71	195	42	22	11
	PAL67 2-7	57	175	44	25	11
	PAL67 2-8	43	180	40	22	10
	PAL67 2-9	29	205	59	29	15
	PAL68 2-5	57	173	29	17	7
	PAL68 2-6	43	177	31	18	8
	PAL68 2-7	29	183	62	34	16
	PAL69 2-2	57	175	49	28	12
	PAL69 2-3	43	159	45	28	11

¹Percentage location based on Nissl-stained sections. The caudal-to-rostral extent of the MGB was assessed by assigning the first caudal section in which the MGB was visible to 0% and the last rostral section in which the MGB was visible to 100%.

mice (Bruckner et al., 1994; Budinger et al., 2000; De Biasi et al., 1994). The macaque monkey is similar to

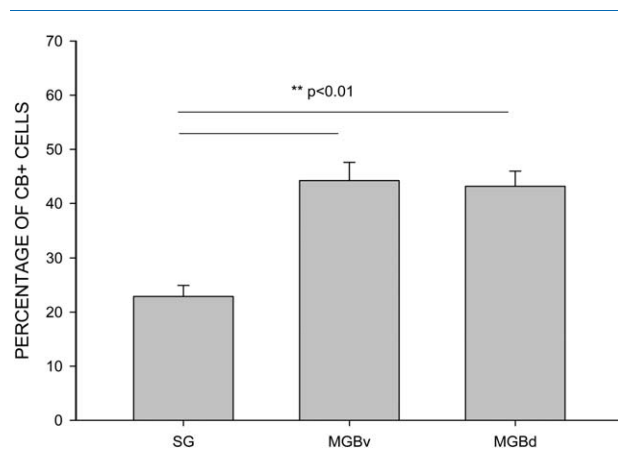


Figure 9. Quantification of percentage of CB⁺ cells relative to Nissl⁺ cells in the different regions of the MGB. The percentage of CB⁺ cells was significantly lower in the SG compared with the MGBd and MGBv. There was no difference between the MGBd and MGBv. The data for this figure are shown in Table 3.

rodents and rabbits in that PV expression is strong and CB expression is weak in the cells of the MGBv (Hashikawa et al., 1991; Molinari et al., 1995). However, the monkey differs from rodents and rabbit in that PV⁺ cells are also common in the MGBd. More PV⁺ cells than CB⁺ cells are found in the anterodorsal MGB of the macaque. Similar numbers of PV⁺ and CB⁺ cells are found in the posterodorsal MGB.

Horseshoe bat and mustached bat are two species of bats in which PV/CB expression in the MGB has been studied (Vater and Braun, 1994; Zettel et al., 1991). Both species are called *constant frequency-frequency modulation* (CF-FM) bats that are obligate echolocators (use echolocation for obstacle avoidance and prey tracking). In general, the PV expression patterns in the MGB of these bats are similar to each other and to those of the macaque monkey but differ from those of rodents and rabbits. PV⁺ cells and neuropil staining are found in both MGBv and MGBd (including the SG). CB⁺ cells are also found in both MGBv and MGBd in these bats. CB⁺ cells are absent in the SG of the mustached bat. The pallid bat differs

from the other species examined (including bats) in terms of PV expression in the MGB. PV staining is absent in the MGBv and is constrained to only the SG. In fact, PV staining appears to be a suitable method to demarcate the SG from other areas of the MGB. Even in the SG, the staining was diffuse, with only a few PV⁺ cells found in some sections (e.g., Fig. 7B). The vast majority of the sections through the SG showed no PV⁺ cells. As in the CF-FM bats, but different from other species, expression of CB in the pallid bat is similar in MGBd and MGBv. However, similarly to the mustached bat, there appears to be reduced expression of CB in the SG in the pallid bat.

Taken together, comparative data do not support a general mammalian plan for expression of PV and CB in the MGB. The only trend is that there is stronger PV than CB expression in the MGBv of

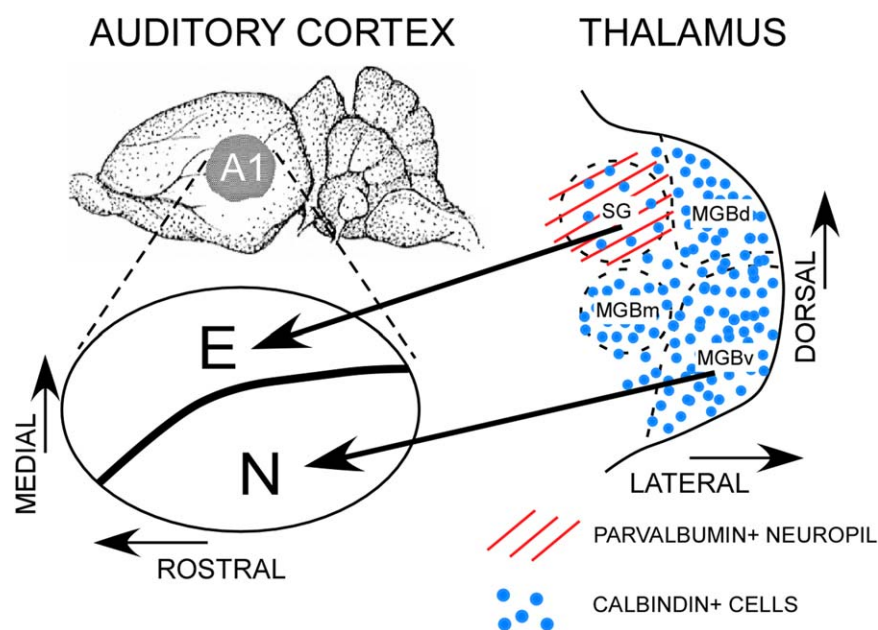


Figure 10. Parallel pathways used in different behaviors show distinct staining patterns for calbindin and parvalbumin. The pallid bat thalamocortical connections contain two parallel pathways: 1) from the supragenicular (SG) nucleus in the MGB to the echolocation call-selective (E) auditory cortical region and 2) from the ventral MGB (MGBv) to the noise-selective (N) cortical region. These pathways likely serve echolocation for obstacle avoidance and passive localization of ground-dwelling prey (e.g., crickets), respectively. At the level of the MGB, these two functional pathways show differential patterns of staining for the calcium binding proteins parvalbumin (PV) and calbindin (CB). The most surprising finding is the virtual lack of PV⁺ neurons in any division of the MGB. Only in the SG was PV staining seen, and that only in the neuropil. CB⁺ cells were present throughout the MGB, but the density was significantly lower in the SG compared with the other MGB regions. [Color figure can be viewed in the online issue, which is available at wileyonlinelibrary.com.]












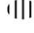




















Species	MGBv		MGBd		SG	
	PV	CB	PV	CB	PV	CB
Rabbit					none	
Rat					?	?
Mouse					?	?
Macaque monkey				* 	?	?
Mustached bat						none
Horseshoe bat						
Pallid bat	none		none		** 	

Figure 11. Comparison of PV/CB expression patterns in the MGB across species. The size of the circle indicates qualitative strength of staining (number of cells or strength of neuropil staining). The solid circumference indicates presence of cell body staining. Absence of a solid circumference line indicates mostly neuropil/fiber staining. Question mark indicates unclear. *None* indicates absence of staining. *In the monkey, there are differences between the anterodorsal and posterodorsal areas of the MGB. **In the vast majority of the sections through the SG of the pallid bat (this study), there were no PV-immunopositive cells. We therefore indicate no cell staining in the SG of the pallid bat. It is important to note that the size of the circles does not indicate similarity of absolute numbers/percentage of stained cells across species; it is intended only to show the relative levels of CB vs. PV staining within each species.

nonchiropterans but not in chiropterans. The functional significance of the species-specific CB/PV expression pattern is unclear. One possibility is that PV expression is higher in thalamic targets of central inferior colliculus (ICc) projection (de Venecia et al., 1995). In support of this suggestion, MGBd in bats shows ICc inputs and high PV expression (Wenstrup et al., 1994). Likewise, the SG in the pallid bat also receives input from the ICc (Razak and Fuzessery, unpublished observations). However, this does not explain the high number of PV⁺ cells in the MGBd of the monkey or the lack of PV expression in the MGBv of the pallid bat. A second possibility is that PV/CB expression correlates with cellular metabolic demands (Braun et al., 1985; Celio et al., 1986) or temporal processing requirements. In echolocating bats, both the MGBd and the MGBv exhibit adaptations for echolocation signal processing (Wenstrup, 1999; Wenstrup and Grose, 1995). During the approach phase of hunting (terminal buzz), many bat species echolocate at a high rate. The homogenous and relatively high expression levels of PV in both MGBv and MGBd in the mustached and horseshoe bat may therefore be a specialization for the metabolic and/or neural temporal fidelity demands of rapid echolocation call processing. The pallid bat data support this suggestion in that the SG, but not the MGBv, appears to be used in echolocation call processing and shows PV expression.

Auditory cortex. Data from rodents, monkeys, and rabbits show that cortical areas with MGBv input strongly express PV. This suggests that MGBv input is correlated with PV expression. Alternatively, cortical PV expression may be an intrinsic property of the primary auditory cortex based on processing requirements such as selectivity for rapid temporal modulations (Atencio and Schreiner, 2008) and/or metabolic demands. The pallid bat data do not support the hypothesis that MGBv input is necessary for high cortical PV expression. The echolocation call- and noise-selective cortical regions are overlain on a tonotopic map of the pallid bat's audible range (6–70 kHz). Together with tonotopy, the short latency and narrowly frequency tuned responses of both areas indicate that they constitute the primary auditory cortex in this species, but only the noise-selective region (5–35 kHz) receives input from MGBv. Thus, if MGBv input was necessary for PV expression, only the noise-selective region part of the primary auditory cortex would show such expression. However, both FM- and noise-selective cortical regions contain similar number of PV⁺ cells. The present study also showed that both PV⁺ and CB⁺ cells were seen in similar numbers in layers I–IV but that PV expression was stronger than CB expression in the deeper layers. In the mouse cortex, more intense CB labeling is seen in the superficial layers compared with the deeper

layers (Cruikshank et al., 2001; Hof et al., 1999). A PV⁺ circuit linking the MGBv and the primary auditory cortex seen in the rabbit (de Venecia et al., 1998) is absent in the noise-selective pathway but may be present in the FM-selective pathway in the pallid bat. Future studies will examine this possibility. Together, these data indicate species-specific patterns in the expression of calcium binding proteins in the auditory thalamocortical pathways.

CONCLUSIONS

Bat species use diverse foraging strategies. Broad classification schemes of bats have focused on the type of echolocation calls used (CF-FM vs. FM bats) or the relative importance of passive vs. active hearing in prey localization. The neuroanatomical and neurophysiological adaptations for various foraging strategies are understood for only a few species. The two CF-FM bats (mustached and horseshoe bat) studied show more similarities to each other than to the pallid bat in terms of calcium binding protein expression in the MGB. All three species belong to different families (mustached bat: Mormoopidae, horseshoe bat: Rhinolophidae, pallid bat: Vespertilionidae). It remains unclear whether the differences in calcium binding protein expression are related to foraging strategy (obligate echolocators vs. passive gleaner) and/or other factors such as the different types of echolocation calls used. Comparative studies of bats, including bats that depend on gleaning to different extents across families, will shed light on the functional basis for differential patterns of calcium binding protein expression and on the convergent neural adaptations for gleaning.

ACKNOWLEDGMENTS

We thank the members of the Razak laboratory for valuable discussion. We also thank Dr. Harpreet Sidhu and Dr. Iryna Ethell for their assistance with the Western blot analysis.

CONFLICT OF INTEREST STATEMENT

We declare that there has been no conflict of interest, including financial, personal, or other relationships with other people or organizations, within 3 years of the original submission.

ROLE OF AUTHORS

All authors had full access to all the data in the study and take responsibility for the integrity of the data and the accuracy of the data analysis. Study concept and design: HMC, KAR. Acquisition of data: HMC, KM. Analysis and interpretation of data: HMC, KM, KAR.

Drafting of the manuscript: HMC, KM, KAR. Critical revision of the manuscript for important intellectual content: KM, KAR. Statistical analysis: HMC, KM, KAR. Obtained funding: KAR. Study supervision: KAR.

LITERATURE CITED

- Atencio CA, Schreiner CE. 2008. Spectrotemporal processing differences between auditory cortical fast-spiking and regular-spiking neurons. *J Neurosci* 28:3897–3910.
- Baimbridge KG, Celio MR, Rogers JH. 1992. Calcium-binding proteins in the nervous system. *Trends Neurosci* 15:303–308.
- Barber JR, Razak KA, Fuzessery ZM. 2003. Can two streams of auditory information be processed simultaneously? Evidence from the gleaning bat *Antrozous pallidus*. *J Comp Physiol A Neuroethol Sens Neural Behav Physiol* 189:843–855.
- Bell GP. 1982. Behavioral and ecological aspects of gleaning by the desert insectivorous bat, *Antrozous pallidus* (Chiroptera: Vespertilionidae). *Behav Ecol Sociobiol* 10:217–223.
- Bennett-Clarke CA, Chiaia NL, Jacquin MF, Rhoades RW. 1992. Parvalbumin and calbindin immunocytochemistry reveal functionally distinct cell groups and vibrissa-related patterns in the trigeminal brainstem complex of the adult rat. *J Comp Neurol* 320:323–338.
- Braun K, Scheich H, Schachner M, Heizmann CW. 1985. Distribution of parvalbumin, cytochrome oxidase activity and ¹⁴C-2-deoxyglucose uptake in the brain of the zebra finch. *Cell Tissue Res* 240:101–115.
- Bruckner G, Seeger G, Brauer K, Hartig W, Kacza J, Bigl V. 1994. Cortical areas are revealed by distribution patterns of proteoglycan components and parvalbumin in the Mongolian gerbil and rat. *Brain Res* 658:67–86.
- Budinger E, Heil P, Scheich H. 2000. Functional organization of auditory cortex in the Mongolian gerbil (*Meriones unguiculatus*). IV. Connections with anatomically characterized subcortical structures. *Eur J Neurosci* 12:2452–2474.
- Celio MR, Scharer L, Morrison JH, Norman AW, Bloom FE. 1986. Calbindin immunoreactivity alternates with cytochrome c-oxidase-rich zones in some layers of the primate visual cortex. *Nature* 323:715–717.
- Cruikshank SJ, Killackey HP, Metherate R. 2001. Parvalbumin and calbindin are differentially distributed within primary and secondary subregions of the mouse auditory forebrain. *Neuroscience* 105:553–569.
- De Biasi S, Arcelli P, Spreafico R. 1994. Parvalbumin immunoreactivity in the thalamus of guinea pig: light and electron microscopic correlation with gamma-aminobutyric acid immunoreactivity. *J Comp Neurol* 348:556–569.
- de Venecia RK, Smelser CB, Lossman SD, McMullen NT. 1995. Complementary expression of parvalbumin and calbindin D-28k delineates subdivisions of the rabbit medial geniculate body. *J Comp Neurol* 359:595–612.
- de Venecia RK, Smelser CB, McMullen NT. 1998. Parvalbumin is expressed in a reciprocal circuit linking the medial geniculate body and auditory neocortex in the rabbit. *J Comp Neurol* 400:349–362.
- Fuzessery ZM, Buttenhoff P, Andrews B, Kennedy JM. 1993. Passive sound localization of prey by the pallid bat (*Antrozous p. pallidus*). *J Comp Physiol A* 171:767–777.
- Gundersen, HJG, Bendtsen, TF, Korbo, L, Marcussen, N, Moller, A, Nielsen, K, Nyengaard, JR, Pakkenberg, B, Sorensen, FB, Vesterby, A, West, MJ. 1988. Some new, simple and efficient stereological methods and their use

- in pathological research and diagnosis. *APMIS* 96:379–394.
- Hashikawa T, Rausell E, Molinari M, Jones EG. 1991. Parvalbumin- and calbindin-containing neurons in the monkey medial geniculate complex: differential distribution and cortical layer specific projections. *Brain Res* 544:335–341.
- Hof PR, Glezer II, Conde F, Flagg RA, Rubin MB, et al. 1999. Cellular distribution of the calcium-binding proteins parvalbumin, calbindin, and calretinin in the neocortex of mammals: phylogenetic and developmental patterns. *J Chem Neuroanat* 16:77–116.
- Jones EG, Dell'Anna ME, Molinari M, Rausell E, Hashikawa T. 1995. Subdivisions of macaque monkey auditory cortex revealed by calcium-binding protein immunoreactivity. *J Comp Neurol* 362:153–170.
- Kosaki H, Hashikawa T, He J, Jones EG. 1997. Tonotopic organization of auditory cortical fields delineated by parvalbumin immunoreactivity in macaque monkeys. *J Comp Neurol* 386:304–316.
- Marsh RA, Fuzessery ZM, Grose CD, Wenstrup JJ. 2002. Projection to the inferior colliculus from the basal nucleus of the amygdala. *J Neurosci* 22:10449–10460.
- Molinari M, Dell'Anna ME, Rausell E, Leggio MG, Hashikawa T, Jones EG. 1995. Auditory thalamocortical pathways defined in monkeys by calcium-binding protein immunoreactivity. *J Comp Neurol* 362:171–194.
- Morest DK. 1964. The neuronal architecture of the medial geniculate body of the cat. *J Anat* 98:611–630.
- Ouda L, Druga R, Syka J. 2008. Changes in parvalbumin immunoreactivity with aging in the central auditory system of the rat. *Exp Gerontol* 43:782–789.
- Rausell E, Jones EG. 1991. Chemically distinct compartments of the thalamic VPM nucleus in monkeys relay principal and spinal trigeminal pathways to different layers of the somatosensory cortex. *J Neurosci* 11:226–237.
- Razak KA. 2011. Systematic representation of sound locations in the primary auditory cortex. *J Neurosci* 31:13848–13859.
- Razak KA. 2012a. Mechanisms underlying azimuth selectivity in the auditory cortex of the pallid bat. *Hear Res* 290:1–12.
- Razak KA. 2012b. Mechanisms underlying intensity-dependent changes in cortical selectivity for frequency-modulated sweeps. *J Neurophysiol* 107:2202–2211.
- Razak KA, Fuzessery ZM. 2002. Functional organization of the pallid bat auditory cortex: emphasis on binaural organization. *J Neurophysiol* 87:72–86.
- Razak KA, Fuzessery ZM. 2006. Neural mechanisms underlying selectivity for the rate and direction of frequency-modulated sweeps in the auditory cortex of the pallid bat. *J Neurophysiol* 96:1303–1319.
- Razak KA, Fuzessery ZM. 2007. Development of functional organization of the pallid bat auditory cortex. *Hear Res* 228:69–81.
- Razak KA, Fuzessery ZM. 2009. GABA shapes selectivity for the rate and direction of frequency-modulated sweeps in the auditory cortex. *J Neurophysiol* 102:1366–1378.
- Razak KA, Fuzessery ZM. 2010. Development of parallel auditory thalamocortical pathways for two different behaviors. *Front Neuroanat* 4.
- Razak KA, Shen W, Zumsteg T, Fuzessery ZM. 2007. Parallel thalamocortical pathways for echolocation and passive sound localization in a gleaning bat, *Antrozous pallidus*. *J Comp Neurol* 500:322–338.
- Razak KA, Zumsteg T, Fuzessery ZM. 2009. Development of auditory thalamocortical connections in the pallid bat, *Antrozous pallidus*. *J Comp Neurol* 515:231–242.
- Rogers J, Khan M, Ellis J. 1990. Calretinin and other CaBPs in the nervous system. *Adv Exp Med Biol* 269:195–203.
- Shen W. 1996. The medial geniculate body of the pallid bat: cytoarchitecture and connectivity with the auditory cortex. Master's Thesis, University of Wyoming.
- Sohal VS, Zhang F, Yizhar O, Deisseroth K. 2009. Parvalbumin neurons and gamma rhythms enhance cortical circuit performance. *Nature* 459:698–702.
- Vater M, Braun K. 1994. Parvalbumin, calbindin D-28k, and calretinin immunoreactivity in the ascending auditory pathway of horseshoe bats. *J Comp Neurol* 341:534–558.
- Wenstrup JJ. 1999. Frequency organization and responses to complex sounds in the medial geniculate body of the mustached bat. *J Neurophysiol* 82:2528–2544.
- Wenstrup JJ, Grose CD. 1995. Inputs to combination-sensitive neurons in the medial geniculate body of the mustached bat: the missing fundamental. *J Neurosci* 15:4693–4711.
- Wenstrup JJ, Larue DT, Winer JA. 1994. Projections of physiologically defined subdivisions of the inferior colliculus in the mustached bat: targets in the medial geniculate body and extrathalamic nuclei. *J Comp Neurol* 346:207–236.
- Wu GK, Arbuckle R, Liu BH, Tao HW, Zhang LI. 2008. Lateral sharpening of cortical frequency tuning by approximately balanced inhibition. *Neuron* 58:132–143.
- Zettl ML, Carr CE, O'Neill WE. 1991. Calbindin-like immunoreactivity in the central auditory system of the mustached bat, *Pteronotus parnelli*. *J Comp Neurol* 313:1–16.